

Microbial metatranscriptomics in a permanent marine oxygen minimum zone

Frank J. Stewart,¹ Osvaldo Ulloa³ and Edward F. DeLong^{2*}

¹*School of Biology, Georgia Institute of Technology, 311 Ferst Drive, Atlanta, GA 30332, USA.*

²*Department of Civil and Environmental Engineering, Massachusetts Institute of Technology, Parsons Laboratory 48, 15 Vassar Street, Cambridge, MA 02139, USA.*

³*Departamento de Oceanografía and Centro de Investigación Oceanográfica en el Pacífico Sur-Oriental, Universidad de Concepción, Casilla 160-C, Concepción, Chile.*

Summary

Simultaneous characterization of taxonomic composition, metabolic gene content and gene expression in marine oxygen minimum zones (OMZs) has potential to broaden perspectives on the microbial and biogeochemical dynamics in these environments. Here, we present a metatranscriptomic survey of microbial community metabolism in the Eastern Tropical South Pacific OMZ off northern Chile. Community RNA was sampled in late austral autumn from four depths (50, 85, 110, 200 m) extending across the oxycline and into the upper OMZ. Shotgun pyrosequencing of cDNA yielded 180 000 to 550 000 transcript sequences per depth. Based on functional gene representation, transcriptome samples clustered apart from corresponding metagenome samples from the same depth, highlighting the discrepancies between metabolic potential and actual transcription. BLAST-based characterizations of non-ribosomal RNA sequences revealed a dominance of genes involved with both oxidative (nitrification) and reductive (anammox, denitrification) components of the marine nitrogen cycle. Using annotations of protein-coding genes as proxies for taxonomic affiliation, we observed depth-specific changes in gene expression by key functional taxonomic groups. Notably, transcripts most closely matching the genome of the ammonia-oxidizing archaeon *Nitrosopumilus maritimus*

dominated the transcriptome in the upper three depths, representing one in five protein-coding transcripts at 85 m. In contrast, transcripts matching the anammox bacterium *Kuenenia stuttgartiensis* dominated at the core of the OMZ (200 m; 1 in 12 protein-coding transcripts). The distribution of *N. maritimus*-like transcripts paralleled that of transcripts matching ammonia monooxygenase genes, which, despite being represented by both bacterial and archaeal sequences in the community DNA, were dominated (> 99%) by archaeal sequences in the RNA, suggesting a substantial role for archaeal nitrification in the upper OMZ. These data, as well as those describing other key OMZ metabolic processes (e.g. sulfur oxidation), highlight gene-specific expression patterns in the context of the entire community transcriptome, as well as identify key functional groups for taxon-specific genomic profiling.

Introduction

Oxygen minimum zones (OMZs) play critical roles in marine community structuring and global biogeochemical cycling. Forming at intermediate depths (~100–1000 m) in response to high biological oxygen demand and reduced ventilation, OMZs occur naturally in zones of nutrient-rich upwelling but are also expanding throughout the world's oceans as a result of anthropogenic effects, such as enhanced nutrient run-off and climate change (Stramma *et al.*, 2006; Diaz and Rosenberg, 2008). This expansion critically impacts marine ecosystems, as OMZs, in which dissolved O₂ often falls below 10 µM, displace oxygen-respiring macroorganisms (e.g. fish) and create anaerobic, microbially dominated communities whose members exert important effects on marine nitrogen and carbon cycles (Ulloa and Pantoja, 2009).

Oxygen minimum zone communities are typified by a low diversity and abundance of pelagic macrofauna but a complex microbial community adapted to life along the oxic–anoxic gradient. Notably, OMZ-associated bacteria and archaea mediate oceanic fixed nitrogen loss to the atmosphere through denitrification and the anaerobic oxidation of ammonia to N₂ (anammox) (Codispoti *et al.*, 2001; Kuypers *et al.*, 2005; Ward *et al.*, 2009). OMZs also play significant roles in greenhouse gas cycling, for example, through the release of the potent heat-trapping

Received 26 August, 2010; accepted 11 November, 2010. *For correspondence. E-mail delong@mit.edu; Tel. (+617) 253 5271.

gas nitrous oxide (N₂O). Recent genetic and biogeochemical evidence also suggests a role for pelagic sulfur cycling in OMZs, mediated in part by the dissimilatory metabolism of sulfur-oxidizing bacteria related to endosymbionts of deep-sea bivalves (Stevens and Ulloa, 2008; Lavik *et al.*, 2009; Walsh *et al.*, 2009; Canfield *et al.*, 2010).

Studies of the Eastern Tropical South Pacific (ETSP) OMZ off northern Chile and Peru have been critical in identifying the organisms and metabolisms characteristic of life in pelagic low oxygen environments. In the ETSP-OMZ, persistent upwelling of nutrient-rich waters drives high primary production in the photic zone (Daneri *et al.*, 2000). As photosynthetically derived organic matter sinks, it is respired and degraded by aerobic heterotrophs, drawing oxygen down from > 200 µM at the surface to less than 1 µM below the oxycline (~50–100 m). Throughout the core of the OMZ (~70–500 m), oxygen decreases to nM concentrations, or even to anoxia (Revsbech *et al.*, 2009). Oxygen conditions remain depleted throughout the year, creating one of the largest persistently oxygen-deficient regions in the global ocean.

As oxygen declines, anaerobic metabolism becomes increasingly important, significantly altering nutrient and organic matter profiles relative to aerobic zones. Notably, oxidized nitrogen species dominate as oxidants in dissimilatory respiration by both autotrophs and heterotrophs. Autotrophic bacteria within the Planctomycetes have been described in the ETSP-OMZ as the primary group responsible for anammox, the likely predominant pathway for fixed nitrogen loss in this system (Thamdrup *et al.*, 2006; Hamersley *et al.*, 2007; Galán *et al.*, 2009; Lam *et al.*, 2009). However, heterotrophic denitrification, the oxidation of organic matter via a complete sequential reduction of nitrate (NO₃) to N₂, also occurs in the ETSP-OMZ (Farías *et al.*, 2009), potentially producing ammonia (via organic matter remineralization) and nitrite (via nitrate reduction) for anammox. Although the range of microorganisms mediating denitrification is not fully described, the multiple steps of this pathway likely involve diverse taxonomic groups. Notably, the dissimilatory reduction of oxidized nitrogen species may involve chemoautotrophic sulfur-oxidizing bacteria. Indeed, genomic analysis of the lineage SUP05, a free-living gammaproteobacterial relative of clam endosymbionts sampled from a North Pacific seasonal OMZ, revealed enzymes necessary for the chemolithotrophic oxidation of reduced sulfur, as well as those for nitrate reduction to nitrous oxide (N₂O), suggesting a mechanistic link between pelagic sulfur cycling and denitrification (Walsh *et al.*, 2009). Symbiont-like 16S rRNA gene sequences have been detected in the ETSP-OMZ, suggesting similar processes at work in this system (Stevens and Ulloa, 2008). Additionally, aerobic ammonia oxidation to nitrite (nitrification) along the oxycline and in

the upper OMZ is intrinsically linked to the dissimilatory nitrogen transformations at the OMZ core, potentially serving as a vital source of nitrite for anammox and fueling an influx of fixed carbon to the system (Lam *et al.*, 2007; Molina and Farías, 2009). Genetic evidence shows a complex nitrifier community in the ETSP-OMZ composed of both bacteria and archaea, although the relative contributions of these two groups to ammonia-oxidation remain unclear (Molina *et al.*, 2007; 2010).

Our knowledge of these diverse OMZ metabolisms is based largely on studies of individual pathways (e.g. denitrification, anammox) or taxonomic groups, or on single-gene surveys of phylogenetic (e.g. 16S rRNA) diversity and functional gene abundance (e.g. nitrite reductase, ammonia monooxygenase). However, we know little of the extent to which specific metabolic processes are represented in the exceedingly diverse pool of genes expressed across a complex microbial community. Community-wide analysis of microbial gene expression in natural communities can help identify unforeseen linkages among metabolic processes (McCarren *et al.*, 2010), as well as inform predictions of the relative synchrony between metabolic transformations and DNA, RNA, and protein abundance in diverse microbial assemblages. Here, we present the first survey of pelagic microbial community gene expression (the metatranscriptome) in an OMZ, focusing specifically on the ETSP-OMZ off northern Chile.

High throughput sequencing of the metatranscriptome has provided an unprecedented overview of gene expression in natural microbial communities, but thus far has been restricted to a handful of aerobic marine environments (Frias-Lopez *et al.*, 2008; Hewson *et al.*, 2009; 2010; Poretsky *et al.*, 2009; Shi *et al.*, 2009). Here, we use pyrosequencing to analyse the community RNA and DNA from four depths spanning the aerobic photic zone (50 m), the oxic–anoxic transition zone (85, 110 m) and the anoxic OMZ core (200 m) at a site on the continental slope. Using BLAST-based characterizations of protein-coding genes, we characterize dominant patterns in metatranscriptome diversity, transcriptional activity and sample relatedness, as well as identify key trends in taxonomic and functional gene representation. These datasets facilitate comparative analysis of bacterioplankton gene expression across diverse oceanic regions, as well as intensive exploration of cryptic, but functionally important, metabolic processes, genes and organisms specific to low-oxygen marine environments.

Results and discussion

Chemical profiles

Vertical profiles of oxygen and inorganic nitrogen at the sampling site (Station #3, ~1050 m depth; ~30 km north-

west of Iquique, Chile; see map in Fig. S1A) resembled those described previously for the ETSP off northern Chile (e.g. Farías *et al.*, 2007; Galán *et al.*, 2009) (Fig. S1B). Oxygen dropped from ~230 μM at the surface to ~100 μM near the base of the photic zone (50 m, mid-oxycline), before falling to ~10 μM at the upper boundary of the OMZ (85 m). Within the OMZ core, oxygen hovered near the level of detection with standard oceanographic oxygen sensors, before gradually increasing again below 500 m. Consistent with prior reports (Farías *et al.*, 2007), nitrite began increasing below the oxycline, reaching a broad maximum (> 6 μM) near the core of the OMZ (200 m). Nitrate peaked initially at the base of the oxycline (~15 μM), decreased gradually in the upper OMZ, then began increasing again near the core of the OMZ. Ammonium concentrations were low along the profile, rising to ~0.35 μM in the centre of the oxic zone before falling to near the limit of detection within the OMZ.

Descriptive statistics of community RNA and DNA

Despite rapid advances in sequencing technology, microbial metatranscriptome studies are still relatively rare, with only a handful of these studies also providing coupled metagenomic samples (Frias-Lopez *et al.*, 2008; Ulrich *et al.*, 2008; Shi *et al.*, 2009; McCarren *et al.*, 2010). As these methods are increasingly applied to diverse ecosystems, it is important to describe general features of the microbial metatranscriptome. We therefore provide statis-

tics describing gene diversity, gene hit count distributions and relatedness among samples both to establish a framework for ecosystem-specific questions and to build a general understanding of gene expression in natural microbial communities.

Read statistics. Pyrosequencing (Roche 454 FLX technology) of community DNA and RNA across four depths generated 1.9 and 1.6 million sequence reads, respectively, with mean lengths of 251 bp and 172 bp (Table 1). Of the RNA reads, 37–61% matched ribosomal RNA sequences and were excluded from further analysis. Given the relatively high abundance of archaea in the samples (see below), further depletion of rRNA would likely have been possible if archaea-specific probe sets were included in the subtractive hybridization protocol used here to deplete rRNA (Stewart *et al.*, 2010). Of the non-rRNA-encoding reads, roughly two-thirds of the DNA reads and one-third of the RNA reads matched protein-coding genes (bit score > 50) in the NCBI-nr database, with similar fractions matching the KEGG database (Table 1). The lower overall percentage of identifiable reads in the RNA data suggests large numbers of non-protein-coding, non-ribosomal RNA transcripts; a similar observation was made in a study showing abundant non-coding small RNAs (smRNA) in bacterioplankton transcriptomes from the subtropical North Pacific (Shi *et al.*, 2009), suggesting a need for characterization of the potentially unique smRNA pool in the OMZ community.

Table 1. Read numbers and statistics.

	DNA				RNA			
	50 m	85 m	110 m	200 m	50 m	85 m	110 m	200 m
Total reads	393 403	595 662	403 227	516 426	379 333	184 386	557 762	441 273
Mean length (bp)	257	253	244	250	183	206	163	173
Mean GC%	38.1	38.2	40.2	41.2	49.2	50.3	47.2	49.6
rRNA reads ^a	1 781	1 887	1 114	1 355	230 593	108 059	204 922	198 584
Mean length (bp)	261	262	249	265	195	221	186	191
Mean GC%	48.0	46.7	47.8	46.3	52.2	51.7	51.8	51.7
Non-rRNA reads ^b	340 117	567 772	380 057	485 044	117 760	69 200	268 093	149 699
Mean length (bp)	256	253	243	249	168	190	165	168
Mean GC%	37.7	38.0	39.9	41.1	43.5	47.6	43.5	46.5
Nr reads ^c	204 953	341 350	215 217	274 463	42 327	16 960	81 492	39 218
Unique nr refs ^d	125 121	177 856	127 767	139 262	32 819	12 567	49 540	30 096
Mean reads per ref ^e	1.6	1.9	1.7	2.0	1.3	1.3	1.6	1.3
Unique nr taxa ^f	4 028	4 696	4 043	4 053	3 183	1 994	3 465	2 838
Mean reads per taxa ^g	51	73	53	68	13	9	24	14
KEGG reads ^h	216 497	329 570	211 024	273 709	38 409	15 430	71 847	33 779

a. Reads matching (bit score > 50) SSU or LSU rRNA sequences via BLASTN.

b. Non-rRNA reads; duplicate reads (reads sharing 100% nucleotide identity and length) excluded.

c. Reads matching (bit score > 50) protein-coding genes in the NCBI-nr database (as of November 26, 2009).

d. Unique NCBI-nr references (accession numbers) identified as top BLASTX hits with bit scores > 50; for reads with multiple top hits of the same bit score, all top hit references are included.

e. Nr reads/unique nr refs.

f. Unique NCBI-nr taxonomic identifiers of top BLASTX hits; ~0.6–1.0% of unique nr references contained no taxonomic identification.

g. Nr reads/unique nr taxa.

h. Reads matching (bit score > 50) genes in the KEGG database (as of February 2009).

Table 2. Protein-coding gene diversity and evenness.^a

	DNA		RNA	
	1/D	E	1/D	E
50 m	10 707	0.694	689	0.049
85 m	9 427	0.634	70	0.006
110 m	12 191	0.767	258	0.020
200 m	8 413	0.575	2008	0.152

a. Values are calculated for subsets of randomly selected protein-coding sequencing reads, standardized to 15 000 reads per DNA/RNA sample.

1/D = Simpson's diversity, where $D = \sum P_i^2$, and P_i is the proportion of the total number of protein-coding sequences represented by the i th unique sequence (accession number).

E = evenness = $(1/D)/S$, where S is the total number of unique sequences per sample; range = 0 to 1, where 1 implies uniform equal counts per unique reference sequence.

Protein-coding gene diversity and distributions. The protein-coding gene sets were highly diverse, encompassing a total of 436 410 unique nr reference sequences representing 7875 taxonomic identifiers (DNA + RNA combined). Of the reference sequences, only 0.2% were present in all datasets (Table S1), and only 4.2% of unique transcripts were detected in the expressed gene pool at all depths. In both the DNA and RNA datasets, the vast majority (> 85%) of reference sequences were represented by fewer than two reads (Fig. S2). The proportional abundance of each gene was highly variable within the RNA samples (low evenness; Table 2). Calculated for sequence subsets standardized to a uniform sample size ($n = 15\,000$), evenness was significantly lower across all RNA samples compared with DNA, falling to a minimum (0.06) in the 85 m sample (upper OMZ) before increasing with depth into the anoxic zone (110 and 200 m). Low evenness in the metatranscriptome was driven by small numbers of highly expressed genes (Fig. S3). Here, 13–30% of all identifiable protein-coding transcripts were represented by the 100 most abundant genes. Indeed, a single gene, encoding an ammonium transporter of the nitrifying crenarchaeote *Nitrosopumilus maritimus*, represented over 8% of the coding transcript pool in one sample (85 m; Fig. S3; Table S5). In contrast, the most abundant genes in the DNA samples never exceeded 0.1% of the total (Table S5). The over-abundance of highly expressed genes in metatranscriptomic samples presents an obstacle to obtaining statistically significant sequence coverage of low frequency transcripts.

Shared gene content. Shared gene content was used to assess the relatedness between sample pairs. To calculate pairwise shared gene percentages and avoid bias as a result of variation in dataset size (i.e. large datasets share more reference sequences in common than smaller datasets), subsets of reads were randomly extracted from

each dataset, yielding uniform numbers of unique nr references per dataset (mean: 12 606; stdev = 0.3%; Table S2). On average, in DNA vs. DNA pairwise comparisons, only 14.7% of reference sequences (per dataset) were shared between depths. A comparable percentage (mean: 13.2%) was shared between RNA samples, similar to values reported for metatranscriptome samples from two photic zone depths in the subtropical North Pacific (Stewart *et al.*, 2010). Comparisons of DNA with RNA datasets, however, revealed significantly lower percentages of shared genes (mean: 8.8%; $P < 0.01$, t -test). Clustering using shared gene percentage as a similarity metric, as in Snel and colleagues (1999), confirmed that each RNA sample was on average more closely related to any other RNA sample than to its corresponding DNA sample from the same depth (Table S2), potentially suggesting similarity in expressed gene content despite high physicochemical heterogeneity across depths. However, deeper sequencing will be required to confirm that the observed discrepancy between metagenome and metatranscriptome gene content is not biased by detection of only the most abundant expressed genes.

To further examine sample relatedness, DNA and RNA datasets were hierarchically clustered based on the distribution of reads matching KEGG gene categories and nr taxonomic identifiers (Fig. 1). These analyses revealed several patterns. First, consistent with the results based on shared gene content percentage, DNA datasets clustered apart from RNA datasets. This partitioning indicates that the content of the expressed functional gene pool, as currently detected at this level of sequencing depth, was distinct from that of the total DNA pool and similar across samples, as demonstrated most clearly at the broadest functional category level (KEGG 2; Fig. 1). This pattern is consistent with a previous observation of metabolic functional similarity across surface water metatranscriptomes from geographically diverse open ocean sites (Hewson *et al.*, 2010). However, this clustering pattern may vary depending on the database used for deriving the similarity metric. Indeed, the correlations between RNA samples weakened at finer levels of the KEGG hierarchy (ko gene level) and when the analysis was based not on functional category but on taxonomic identifier (Fig. 1, bottom), although the separation of DNA and RNA samples was maintained. Second, correlations between samples were higher for DNA samples compared with RNA samples, indicating that variation in functional category distributions across depths was greater in the metatranscriptome than in metagenome (Table 2). However, this pattern was violated for the 200 m RNA sample, which more closely resembled the DNA samples in three of the four clustering analyses. This grouping may reflect the transition to the unique microbial community at the core of the OMZ. For example, if the 200 m community was sufficiently distinct

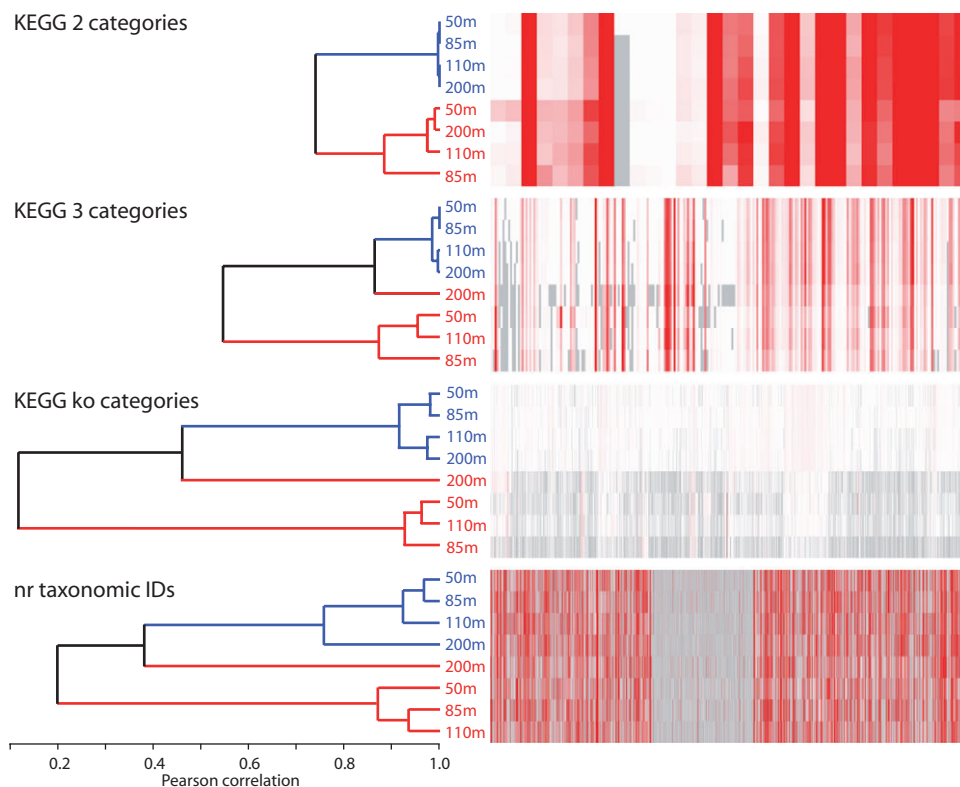


Fig. 1. Relatedness of OMZ DNA and RNA datasets. Heat maps show the relative distribution of protein-coding reads matching gene categories at three levels of the KEGG hierarchy (see Figs S6–S8 for KEGG gene categories) and across NCBI-nr taxonomic identifiers. Gray = missing data; white = low values, red = high values. Dendrograms are based on hierarchical clustering of Pearson correlation coefficients for each pairwise dataset comparison, with blue and red branches highlighting DNA and RNA datasets respectively.

from that of the upper depths, the 200 m RNA sample may be recruited into the DNA cluster based on similarity to its corresponding DNA sample. Finally, the DNA samples showed clear vertical clustering, with the upper samples (50 and 85 m) clustering separately from those of the middle OMZ (110 and 200 m). This pattern suggests depth-specific transitions in community structure, with a distinction between oxycline-associated communities and those from the lower, more oxygen-depleted depths. However, the consistent, independent clustering of DNA and RNA samples suggests that the functional distinction between coupled metagenome and metatranscriptome samples is greater than that among samples from different depths. Deeper sequencing is required to determine whether this pattern holds as more of the metatranscriptome becomes characterized.

Transcriptional activity. The transcriptional activity of protein-coding genes varied marginally with depth in the OMZ. Mean expression ratios (RNA/DNA) calculated across the full datasets showed a spike just below the oxycline (85 m; Fig. 2). However, this pattern was driven primarily, but not exclusively, by variation in sample size

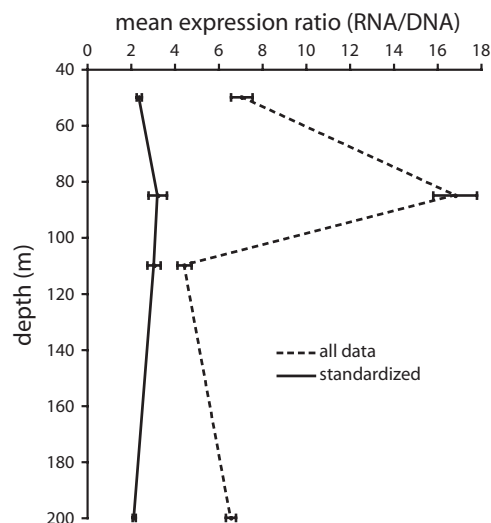


Fig. 2. Expression ratios (RNA/DNA) averaged across all protein-coding genes (NCBI-nr annotations) per depth. 'All data' shows values uncorrected for variation in sample size. 'Standardized' values are calculated for subsets of each full dataset standardized to a common size ($n = 15\,000$ protein-coding reads each). Error bars are 95% confidence intervals.

(total number of protein-coding genes per dataset). At shallower sequencing depths (as in the 85 m RNA sample; Table 1), highly expressed genes occupy a greater proportion of the total number of unique genes detected; as sampling depth increases, low frequency genes occupy a greater proportion of the total and thereby depress the mean expression ratio. After standardizing the datasets to a common size ($n = 15\,000$ protein-coding reads), the increase in expression at 85 m decreased substantially, but remained elevated relative to values in the oxycline and at the OMZ core. It is unclear to what extent transcript abundance serves as a proxy for cellular activity, particularly given the asynchrony frequently observed between transcript and protein levels (e.g. Taniguchi *et al.*, 2010). However, prior reports show that bacterioplankton cell counts reach a secondary local maximum below the oxycline in the OMZ off Iquique (Molina *et al.*, 2005; Galán *et al.*, 2009), potentially supporting a local increase in metabolic activity in this zone.

Taxonomic diversity

Protein-coding gene sequences. The taxonomic identifications of protein-coding genes provide an alternative to ribosomal RNA-based classifications of taxonomy (e.g. Urich *et al.*, 2008). Here, we present results characterized by searches against the extensive NCBI-nr database of protein-coding genes. Searches against nr maximized our chances of identifying functional gene diversity, as well as helped identify close relatives whose annotated genomes might be used to inform more targeted analyses of gene expression dynamics at the genome level. Although the relatively short sequences (~200 bp) obtained via FLX-based pyrosequencing do not lend themselves to comprehensive phylogenetic reconstructions, the annotations of nr functional genes matching these sequences (top BLASTX hit) can be used as an approximate taxonomic classification for each read. Here, nr functional gene annotations revealed depth-specific transitions in microbial community composition and transcription across the OMZ. At all depths, the rank abundances of dominant taxa differed between the DNA and RNA pools (Figs 3 and 4). Assuming the ratio of RNA to DNA abundance of specific genes reflects the relative metabolic activity level, the data suggest several broad trends, supported in part by the high frequency of reads matching several prominent individual taxa (Fig. 5, Tables S3 and S4).

First, metabolic activity along the oxic–suboxic transition zone was dominated by Crenarchaea. Up to one-third of all identifiable protein-coding transcripts from the upper OMZ and within the oxycline matched a crenarchaeote, including numerous uncultured representatives, as well as two ammonia-oxidizing species for which genome data are available: *Cenarchaeum symbiosum*, a marine

sponge symbiont (Preston *et al.*, 1996; Hallam *et al.*, 2006a), and *N. maritimus* (Nm), a cultured nitrifier isolated from a marine aquarium (Konneke *et al.*, 2005; Schleper *et al.*, 2005). In contrast to other well-represented taxonomic groups (e.g. *Pelagibacter*), the proportional representation of crenarchaea was consistently higher in the RNA reads, relative to the DNA, suggesting an active crenarchaeal community at these depths (Fig. 4).

Crenarchaeal genes most highly similar to *N. maritimus* (Nm) dominated these samples, constituting up to 20% of identifiable transcripts (85 m sample) and exhibiting a mean expression ratio 4.5-fold higher than that of the most abundant taxon represented in the DNA (*Pelagibacter*; Figs 3, 4 and S4). Of the protein-coding genes in the Nm genome ($n = 1795$; Walker *et al.*, 2010), 74%, 81% and 56% were recovered as top hits in BLASTX searches of the 50, 85 and 110 m DNA reads, respectively, with relatively uniform coverage across the genome (Fig. 5). A smaller proportion of Nm genes (15–41%) was represented in the transcript pool, likely reflecting (in part) the smaller size of the RNA datasets (Table 1).

These results support prior studies underscoring the ubiquity of crenarchaeal-like Archaea in the global ocean. Hallam and colleagues (2006a) reported a high percentage of DNA sequences closely matching the genome of the crenarchaeal nitrifier *C. symbiosum* (mean 65% amino acid identity) during winter in the Sargasso Sea. A more recent analysis of the suboxic zone of the Black Sea revealed that up to one quarter of all prokaryotic cells fell within a single clade of nitrifying crenarchaea closely related to Nm (Labrenz *et al.*, 2010). Walker and colleagues (2010) recently reported that an average of 1.2% of the sequences present in the Global Ocean Sampling (GOS) database match Nm across diverse physiochemical habitats and geographic locations. In their analysis, the majority of DNA reads mapping to Nm shared > 50% amino acid identity with the reference genome. In our study, reads matched Nm at high identity (mean: 74–75% for DNA, 70–81% for RNA across depths), with the majority of top Nm hits > 75% identical to the reference (median: 76–78% for DNA, 64–84% for RNA). Consistent with previous studies (Hallam *et al.*, 2006a; Walker *et al.*, 2010), our analysis identified several gaps in genome coverage, perhaps indicating regions unique to the cultured strain (Fig. 5). Our data, along with supporting studies, highlight an emerging perspective of crenarchaeal dominance in the pelagic nitrification zone separating oxic from suboxic waters.

Second, protein-coding gene annotations confirm a prominent sulfur-oxidizing microbial community in the ETSP-OMZ. DNA and RNA reads from the OMZ core were particularly enriched in sequences matching the genomes of sulfur-oxidizing endosymbionts (gammaproteobacteria) of deep-sea clams [*Candidatus* Ruthia

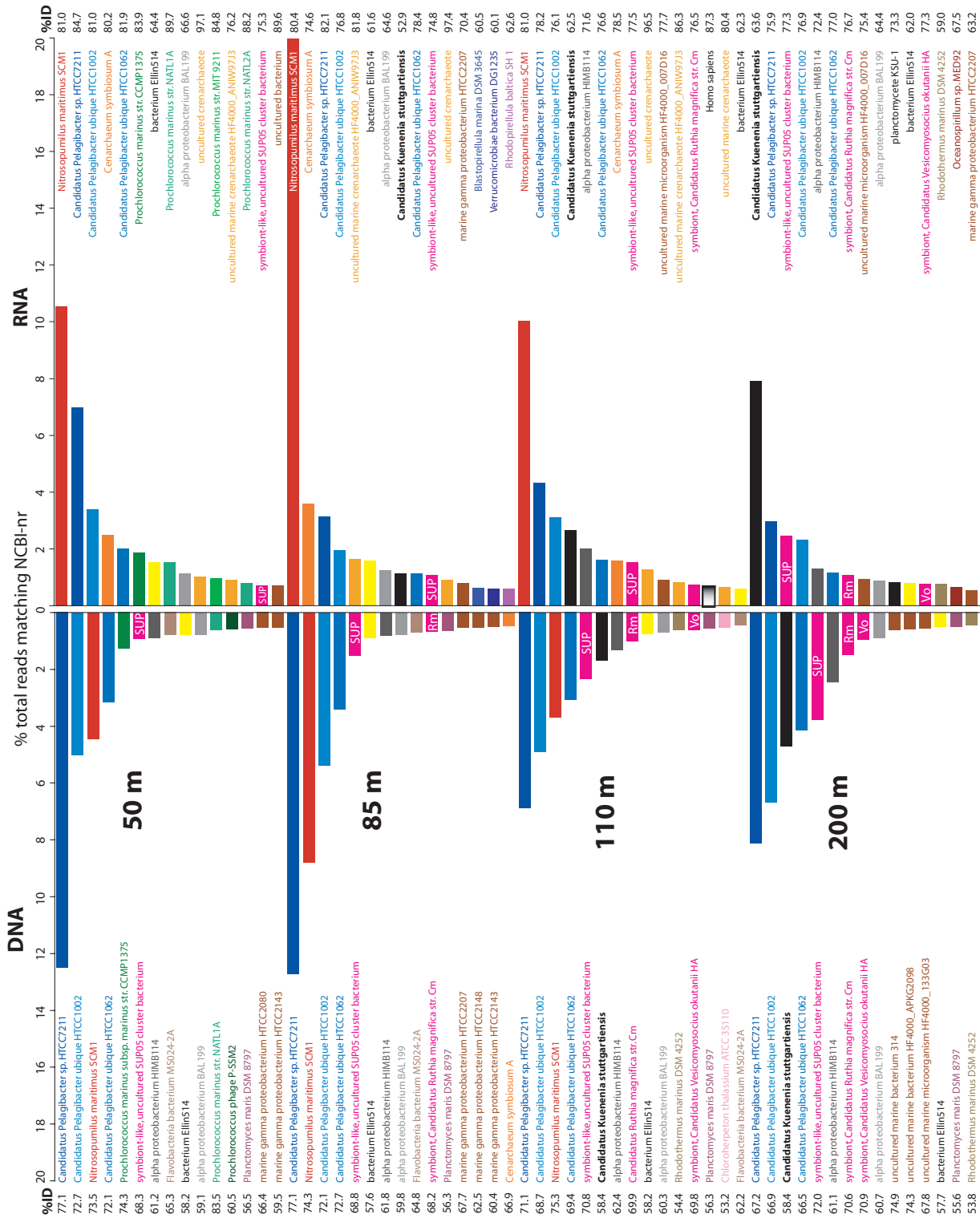


Fig. 3. Community and expression shifts with depth in the OMZ. The fifteen most abundant taxa per depth are identified based on the NCBI taxonomic affiliation of protein-coding genes matching (top blast hit) DNA and RNA sequence reads. Percentages (%ID) adjacent to taxon names are the mean amino similarities across all genes within each taxon, based only on the high-scoring segment pair (HSP) in each statistically significant BLAST alignment. Similarities were averaged per gene, and then across all genes per taxon.

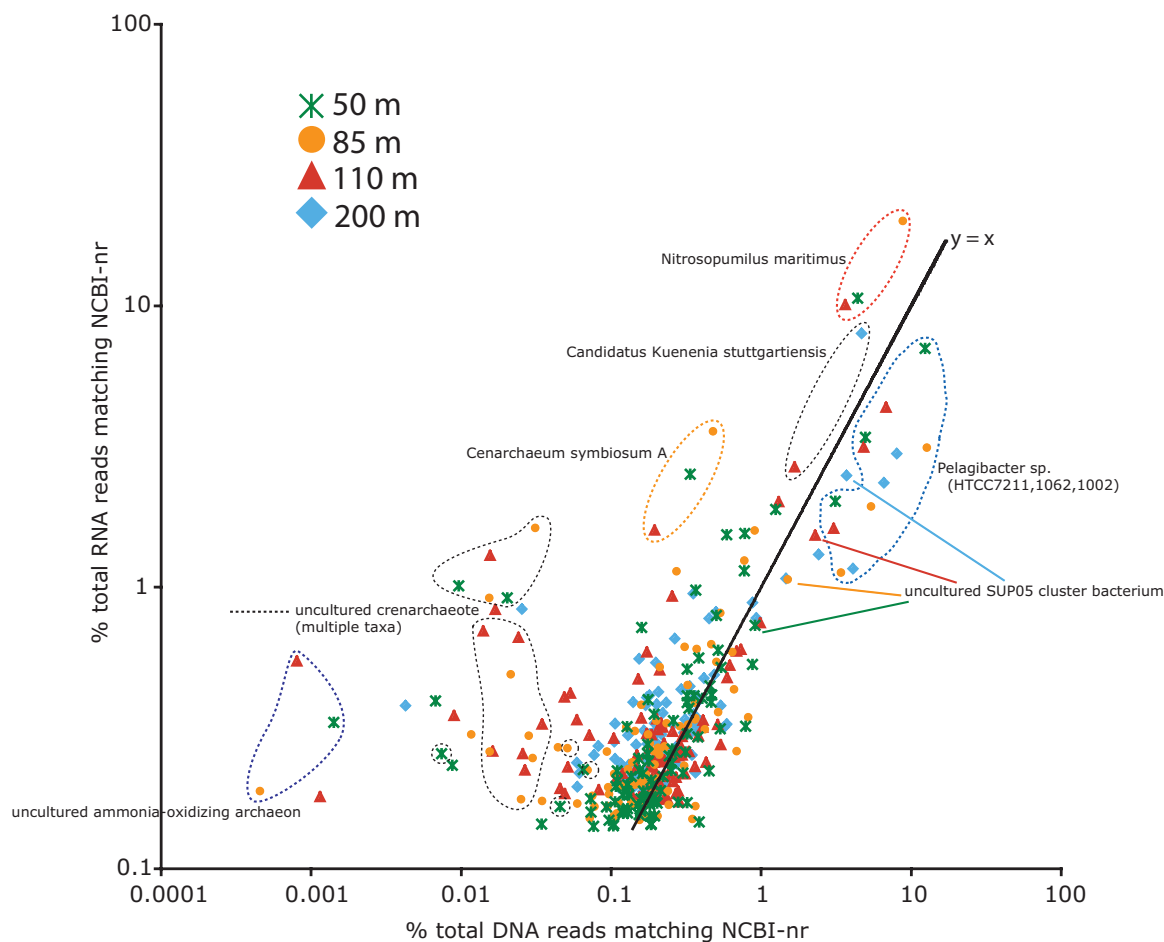


Fig. 4. Relationship between DNA and RNA abundance for dominant OMZ taxa, as identified by the NCBI taxonomic affiliation of protein-coding genes matching sequence reads (as top BLASTX hit in searches against the nr database). Abundances are expressed as percentages of the total number of reads with matches in nr (per dataset); plots show only the 100 most abundant taxa per depth (based on rankings in the RNA). Axis units are log-scaled.

magnifica (Rm) and *Candidatus Vesicomysocius okutanii* (Vo); Kuwahara *et al.*, 2007; Newton *et al.*, 2007] and the symbiont-like SUP05 lineage isolated from a seasonally anoxic fjord off British Columbia (Walsh *et al.*, 2009) (Fig. 3). At all depths, the proportional abundance of these taxa was greater in the DNA than in the RNA, indicating reduced transcriptional activity relative to other groups (e.g. crenarchaea; Fig. 4). These results are consistent with prior genetic and genomic surveys. Indeed, ribosomal RNA gene (16S) sequences related to those from sulfur-oxidizing Rm and Vo endosymbionts have been recovered from diverse low oxygen regions including the ETSP (Stevens and Ulloa, 2008), the coastal North Pacific (Zaikova *et al.*, 2010), the Arabian Sea (Fuchs *et al.*, 2005) and the upwelling zone off Namibia (Lavik *et al.*, 2009). Furthermore, the metagenome of the SUP05 lineage has been sequenced (Walsh *et al.*, 2009), revealing genes required for sulfur oxidation, carbon fixation and nitrate reduction. This metabolically versatile bacterium is

hypothesized to oxidize reduced sulfur via the dissimilatory sulfite reductase (DSR) and sox pathways, using nitrate as a terminal electron acceptor (Walsh *et al.*, 2009). Here, our reads matched a diverse SUP05 gene set at relatively uniform abundance, with 73% of the genes encoded in the SUP05 metagenome detected in the 200 m DNA sample (Fig. 5). Together, these studies confirm that organisms capable of chemolithotrophic oxidation of sulfide, likely with nitrate (Lavik *et al.*, 2009; Walsh *et al.*, 2009), are a common component of pelagic low oxygen environments.

Third, bacteria capable of anaerobic ammonia oxidation (anammox) are common and transcriptionally active at the core of the OMZ. Notably, reads matching the anammox planctomycete *Candidatus Kuenenia stuttgartiensis* (Ks) increased with depth to 7.9% of total nr hits in the 200 m RNA sample, 1.7-fold higher than the proportional representation of Ks in the corresponding DNA (Fig. 3). RNA reads matched a total of 705 distinct Ks genes (out of a

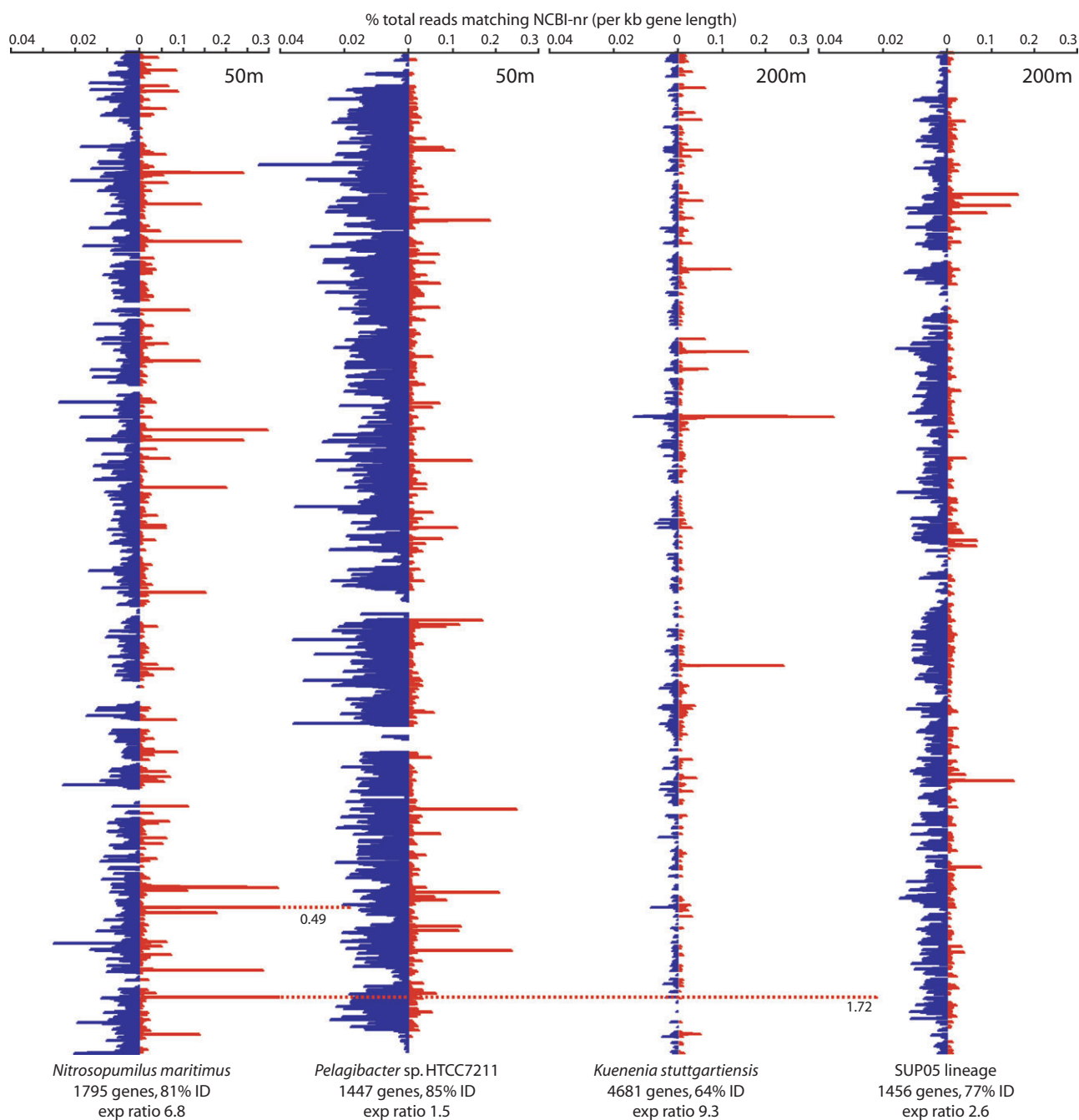


Fig. 5. Distribution and abundances of DNA (blue) and RNA (red) reads with top hits to protein-coding genes in the genomes (or metagenomes) of prominent OMZ taxa: *Nitrosopumilus maritimus* (crenarchaeote, ammonia oxidizer), *Pelagibacter* sp. HTCC7211 (alpha proteobacterium, heterotroph), *Kuenenia stuttgartiensis* (planctomycete, anammox), and the SUP05 lineage (gamma proteobacteria, sulfur oxidizer). Data are shown for the depth at which each taxon was best represented, based on the proportion of genes recovered as top hits in the RNA data (Fig. 3). The total number of protein-coding genes, the mean amino acid sequence similarity of RNA reads matching those genes (ID; mean per gene, averaged across all genes) and the mean expression ratio of genes present in both the DNA and RNA are shown below. Genes are sorted vertically by genome position (*Nitrosopumilus*, *Pelagibacter*) or accession number (*Kuenenia*, SUP05; synteny is therefore not implied for these taxa), with gene abundance (reads per gene as a percentage of total reads matching NCBI-nr genes) normalized per kb of gene length. The most abundant expressed genes and the most highly expressed genes (exp. ratio) per taxon are listed in Tables S3 and S4.

possible 4681; (Strous *et al.*, 2006), with a mean expression ratio of 9.3 per gene, comparable with that recorded for Nm at the oxycline (6.8) and considerably higher than that for SUP05 at the same depth (2.6; Fig. 5). Prior ribosomal RNA gene surveys indicate that the majority of OMZ-associated planctomycetes actually cluster within the marine *Candidatus* Scalindua group (Kuypers *et al.*, 2003; Woebken *et al.*, 2008; Galán *et al.*, 2009), rather than with Ks, which was characterized from a wastewater-fed laboratory bioreactor (Strous *et al.*, 2006). This clustering is consistent with the relatively low mean amino acid identity observed here for reads matching Ks (64%; Figs 3 and 5), likely reflecting the scarcity of planctomycete genome data (e.g. Scalindua spp. protein-coding genes) in the NCBI-nr database.

Finally, several taxa were consistently abundant throughout the OMZ but contributed disproportionately to the total transcript pool. For example, the ubiquitous marine alphaproteobacterial genus *Pelagibacter* dominated the DNA at all depths (15–22% of all identifiable protein-coding genes; Fig. 3), consistent with prior reports based on 16S clone libraries (Stevens and Ulloa, 2008). DNA reads matching a single genotype, *Pelagibacter* sp. HTCC7211 from the oligotrophic Sargasso Sea (Carlson *et al.*, 2009), reached 12% of the total in the 50 and 85 m samples, and covered 89% of the protein-coding genes in the reference genome (Fig. 5). However, the mean expression ratio for HTCC7211 genes in this sample was relatively low (1.5, compared with a sample mean of 2.0) and all *Pelagibacter* species were consistently under-represented in the RNA pool (Figs 1, 4 and S4). This trend emphasizes the potential disconnect between genomic abundance and metabolic activity.

Ribosomal RNA gene sequences. DNA reads matching ribosomal RNA gene sequences constituted a small fraction of the total reads (16S rRNA reads < 1%), but nonetheless provided a broad overview of the relative abundance of higher-level taxonomic groups (Fig. S5). At a general level, patterns in 16S reads paralleled those of the protein-coding DNA pool. Notably, alphaproteobacteria sequences were consistently abundant throughout the OMZ (~1/3 of 16S reads at all depths), reflecting the strong representation of *Pelagibacter* species in the non-rRNA reads. Gammaproteobacteria were equally well represented, although slightly less abundant than reported previously for the OMZ off Iquique (Stevens and Ulloa, 2008). Consistent with a spike in non-rRNA genes matching *Candidatus* Kuenenia stuttgartiensis, planctomycete 16S reads peaked at the core of the OMZ (200 m). Archaea represented less than 15% of 16S sequences at all depths, with crenarchaeal sequences constituting ~5% of 16S reads in the upper OMZ and above the oxycline, then declining in abundance into the suboxic depths. This

pattern parallels the gradient in protein-coding DNA but belies the disproportionately strong expression signal from the crenarchaeal community. A similarly asynchronous signal has been observed in the central Pacific Ocean, where the relative abundance of crenarchaeal ammonia monooxygenase (*amoA*) gene sequences was disproportionately low relative to *amoA* transcript abundance (Church *et al.*, 2010). Such patterns highlight the potential of numerically non-dominant members of the community to contribute significantly to microbial community metabolic activity.

Functional trends

Reads matching NCBI-nr functional genes and KEGG categories provide an overview of the functional processes driving transcriptional activity in the OMZ (see also Figs S6–S11, Tables S5–S8). Exhaustive characterization of the functional genes and pathways represented in our data is beyond the scope of a single analysis. However, several dominant trends emerge from our survey and are highlighted here.

Ammonia oxidation. Transcript distributions underscore a prominent role for crenarchaeal nitrification along the oxic–suboxic transition zone. Crenarchaeal *amo* sequences, encoding the subunits of ammonia monooxygenase (AmoABC) were among the most highly expressed genes in the 50, 85 and 110 m samples, representing 2.7–4.7% of all sequences identified by KEGG searches, exhibiting expression ratios of 85–167 (Table S5, Fig. S8). In contrast to prior studies suggesting a role for bacterial nitrifiers in the Chilean OMZ (Molina *et al.*, 2007; Lam *et al.*, 2009), as well as to our DNA results that show a mixture of both bacterial and archaeal *amo* genes in the OMZ metagenome, the expressed *amo* transcripts were dominated exclusively by crenarchaeal sequences (98–100%; Fig. S9). These data corroborate recent results showing the relative dominance of archaeal *amoA* gene sequences in clone libraries and Q-PCR assays from permanent OMZ sites off Chile and Peru (Molina *et al.*, 2010). Here, transcripts matching Nm *amo* genes were particularly well represented (Table S5). While Nm has been shown experimentally to oxidize ammonia to nitrite, Nm *amo* genes have relatively low similarity to characterized bacterial *amo* genes and may encode a unique functional variant of the enzyme; indeed, other genes involved in nitrification [e.g. hydroxylamine oxidoreductase (HAO)] are lacking from this organism (Konneke *et al.*, 2005; Hallam *et al.*, 2006a,b; Walker *et al.*, 2010). Together, our results confirm a major role for crenarchaeal ammonia-oxidation along the oxycline and into the OMZ, consistent with a growing body of literature describing the ubiquity and potential dominance of

archaeal nitrification in diverse marine habitats (see Wuchter *et al.*, 2006), and references in (Prosser and Nicol, 2008; Erguder *et al.*, 2009).

Ammonium transport. Membrane transport processes predominated in the OMZ metatranscriptome (Figs S6–S8), corroborating prior reports showing the general importance of transport functions in marine bacterioplankton across diverse environments (Frias-Lopez *et al.*, 2008; Sowell *et al.*, 2009; Poretsky *et al.*, 2010). While transcripts encoding ATP-dependent ABC transporters were consistently abundant throughout the OMZ (5–6% of total KEGG hits; Fig. S7), those encoding proton motive force-dependent nitrate transporters (e.g. NarK) increased markedly with depth, paralleling a similar increase in nitrate reductase transcription (see below). In contrast, other ion coupled transporters peaked at the oxycline and in the upper OMZ (Figs S7 and S8), before declining markedly towards the OMZ core. Notably, transcripts encoding an ammonium transporter (Amt) constituted 11% of all reads with matches in the nr database and 18.4% of all reads matching the KEGG database in the 85 m sample (Table S5, Figs S8 and S9). Of the Amt-like reads identified at this depth, 93% matched genes belonging to crenarchaea, with the ammonium transporter of *N. maritimus* (accession ABX13594) representing the single most abundant reference gene across all datasets (Table S5). In contrast, crenarchaea represented only 16% of the Amt-like reads in the DNA pool at this depth, emphasizing the sometimes striking differentiation between gene (or taxonomic) representation and functional expression (Fig. S9).

The mechanistic basis for high Amt expression in the crenarchaeal community is unclear. It is tempting to speculate that active ammonium transport is required to support nitrification (Hallam *et al.*, 2006a,b). Indeed, ammonium accumulation via active transport has been shown for nitrifying bacteria (*Nitrosomonas*), and suggested as a mechanism for meeting internal kinetic requirements for ammonia oxidation when environmental concentrations and passive ammonia diffusion rates are low, as is common in marine environments (Schmidt *et al.*, 2004; Weidinger *et al.*, 2007). However, less is known about Amt function in archaea (Andrade and Einsle, 2007; Leigh and Dodsworth, 2007), and the relative contributions of Amt-based transport to energy metabolism and biosynthesis have not been explored. Interestingly, recent experiments on cultured cells show that *N. maritimus* has a remarkably high affinity for reduced nitrogen, among the highest ever recorded for microbial substrates (Martens-Habbena *et al.*, 2009). This affinity is hypothesized to allow Nm to effectively compete against bacterial nitrifiers, as well as against other marine phototrophs and heterotrophs for ammo-

nium in ammonium-depleted waters. In the ETSP-OMZ, *amt* transcripts paralleled *amo* transcripts in Nm-like crenarchaea, raising the hypothesis that the unprecedented capacity for ammonium acquisition in cultured ammonia-oxidizing crenarchaea may be linked to overexpression of ammonium transporters. However, the extent to which this hypothesis applies to *in situ* conditions in the OMZ is uncertain, as OMZ crenarchaea thrive along the oxycline where ammonium is available and produced at high rates (Fig. S1) (Molina *et al.*, 2010).

Anaerobic nitrogen metabolism. RNA profiles confirmed a significant transition to anaerobic nitrogen metabolism with depth in the OMZ. Genes encoding the multi-subunit dissimilatory nitrate reductase (*nar*), present in both the traditional denitrification pathway and in anammox, were detected at all depths but were proportionately most abundant in the RNA samples (relative to DNA) and at the core of the OMZ (Table S5, Fig. S10). Specifically, *narG*, encoding the alpha subunit of the enzyme, increased with depth to represent 1% of all identifiable protein-coding genes in the 200 m transcriptome. The pattern of *narG* sequence diversity differed substantially between the DNA and RNA pools (Fig. S10). Diverse *narG* sequences were detected at all depths in the DNA, representing between 32 and 389 distinct nr reference genes and suggesting a range of taxa with the capacity for nitrate respiration. In contrast, the *narG* transcript pool was strikingly uniform in the upper OMZ, where all transcripts from the 50 m and 85 m samples matched a single reference sequence, from the anammox planctomycete *Candidatus* Kuenenia stuttgartiensis (Ks; Fig. S10). In contrast, at 200 m the nitrate reductase transcript pool was incredibly diverse, representing 187 distinct nr reference sequences from diverse taxa, including the symbiont-like sulfur oxidizers Vo and SUP05. This transition in transcript diversity highlights a community-wide shift to nitrate as a terminal electron acceptor at the OMZ core (or anammox end product; Strous *et al.*, 2006), emblematic of the high potential denitrifier diversity in OMZs (Castro-González *et al.*, 2005; Jayakumar *et al.*, 2009).

A strong representation of key planctomycete functional genes suggests a prominent role for anammox in the OMZ. Notably, the proportional abundance of transcripts encoding planctomycete hydrazine/HAO, an enzyme critical to the conversion of hydrazine to N₂ during anammox (Kuenen, 2008), increased 300-fold from the 50 m to the 200 m sample, accounting for a maximum of 1.4% of all identifiable protein-coding reads (NCBI-nr matches, summed across multiple taxa). Of these reads, 98% matched sequences annotated as planctomycetes. Planctomycete *narG* sequences, predominantly those matching Ks (see above), were also

well represented, but were proportionately most abundant when planctomycete HAO transcripts were rare (Fig. S10). The molecular basis of the anammox reaction is not completely understood, but likely involves the Nar enzyme acting in reverse to oxidize nitrite to nitrate, pumping electrons into transport systems to fuel autotrophy (Strous *et al.*, 2006; Jetten *et al.*, 2009). However, anammox bacteria may also use Nar to oxidize organic matter with nitrate. Indeed, anammox planctomycetes are much more metabolically diverse than previously thought and have been shown to use organic acids as electron donors to reduce nitrate and nitrite and to out-compete heterotrophic denitrifiers for these substrates (Kartal *et al.*, 2007a,b; 2008).

Sulfur energy metabolism. Transcripts from diverse pathways confirm the activity of sulfur-based energy metabolism in the OMZ (Table S6). Notably, genes of the dissimilatory sulfite reductase enzyme (Dsr), the sulfur oxidation (Sox) gene complex mediating thiosulfate oxidation and the adenosine 5'-phosphosulfate reductase (Apr) were expressed throughout the OMZ (Tables S6–8), with the greatest proportional representation coming from *dsr* genes at the OMZ core. Several of the proteins encoded by these genes, including Dsr and Apr enzymes, function in both oxidative and reductive pathways. Notably, homologues encoding AprBA and DsrAB are present in a wide range of chemolithotrophic sulfur oxidizers, as well as sulfate reducers (Dhillon *et al.*, 2005; Meyer and Kuever, 2007a,b). These genes share ancestry and structure but can be differentiated into distinct phylogenetic clades. Here, the majority (> 90%) of *aprAB* and *dsrAB* transcripts matched genes in NCBI-nr belonging to sulfur-oxidizing organisms, including green and purple sulfur bacteria, the SUP05 lineage and thiotrophic symbionts of diverse hydrothermal vent and seep fauna (Tables S7 and S8). The detection of transcripts encoding the nitrate reductase present in several of these taxa (e.g. SUP05 and the symbiont *Candidatus Vesicomysococcus okutani*; Fig. S10) suggests dissimilatory sulfur oxidation with nitrate in the OMZ and therefore a potential coupling between sulfur oxidation and denitrification in the OMZ. Indeed, recent experimental analyses of water from below the oxycline in the Chilean OMZ demonstrates a direct coupling between sulfide oxidation and nitrate reduction to both nitrite and nitrous oxide (Canfield *et al.*, 2010), consistent with prior suggestions of coupling between marine sulfur and nitrogen cycles in other redox-stratified zones (Jensen *et al.*, 2009; Lavik *et al.*, 2009). In conjunction with these studies, our data indicate an active sulfur cycle in the OMZ, highlighting the need for experimental metatranscriptomic analyses (e.g. bioreactor experiments) in which community sulfur (and nitrogen) metabolism can be directly monitored relative to bio-

chemical rate measurements and in response to environmental perturbations.

These results highlight only a small subset of the exceedingly diverse network of genes expressed in the OMZ. Indeed, further examination of these datasets is warranted, and many interesting trends present in the data will emerge as more complementary datasets accumulate. For example, the relative abundance of transcripts encoding transposases increased 23-fold from the 50 m to the 200 m sample, paralleling a similar increase in the genomic DNA (Fig. S11). Overrepresentation of transposases with depth in DNA has been reported for bacterioplankton in the North Pacific Subtropical Gyre, where transposase abundance in metagenomic libraries increased ~30-fold from the surface to 4000 m (DeLong *et al.*, 2006; Konstantinidis *et al.*, 2009). This trend was shown to parallel a general decrease in purifying selection pressure with depth, leading the authors to hypothesize a causal relationship between relaxed selection and mobile element expansion (Konstantinidis *et al.*, 2009). Although the ultimate factor(s) driving this pattern remain unclear, our data support a global trend in depth-specific mobile element activity that spans both oxic and suboxic conditions. In this coastal OMZ environment, the gradient of mobile element expansion versus depth appears much steeper than in the open ocean. Additional comparative analyses of individual genes and pathways will likely reveal other globally conserved processes operating in the OMZ.

Conclusions

A central challenge in environmental microbiology is to place individual genes and species in the context of the integrated communities in which they operate. High-throughput sequencing of community RNA takes an important step in this direction, providing snapshots in time of the proportional abundance of tens of thousands of diverse transcripts. Here, we present the first survey of an OMZ metatranscriptome, with two broad goals.

First, at a general level, we characterized the sequence diversity and relatedness between coupled metagenomic and metatranscriptomic datasets using descriptive statistics (e.g. evenness) and clustering. Although metatranscriptomic analyses are being increasingly applied to natural microbial communities, only a small number of studies have analysed both DNA and RNA sequence pools in tandem (Frias-Lopez *et al.*, 2008; Urich *et al.*, 2008; Shi *et al.*, 2009). The extent to which current sequencing and analytical methods capture the diversity in these two pools remains poorly described. Here, despite read counts in the hundreds of thousands, minimal overlap in individual gene content occurred between datasets, although clustering based on broader

functional gene categories identified similarity in expressed gene content across samples. The latter may be consistent with a broader trend in functional conservation in the highly expressed gene set (e.g. Hewson *et al.*, 2010), but confirmation of this pattern requires comparative analysis of diverse microbial metatranscriptomes, which so far have been characterized primarily for marine bacterioplankton. In conjunction with prior studies, our results describe the marine microbial metatranscriptome as dominated by small numbers of highly expressed genes (e.g. *amt* genes in this study, as in Frias-Lopez *et al.*, 2008 and Hewson *et al.*, 2010), emphasizing a need for greater sequencing depth to adequately characterize low frequency transcripts, as well as potential functional (or evolutionary) differences among genes with varying expression patterns. Targeted removal of highly expressed protein-coding genes, potentially via modification of existing subtractive hybridization protocols (e.g. Stewart *et al.*, 2010), may enable more comprehensive characterizations of functional diversity in the microbial metatranscriptome.

Second, these datasets provided a snapshot of dominant taxonomic and functional trends in the Chilean OMZ at the time of collection. This analysis was simplified in part by focusing on sequences matching specific organisms diagnostic of key OMZ functions (e.g. nitrate reduction, anammox, sulfur oxidation), an approach facilitated by comparisons against the extensive NCBI-nr database. Notably, these data identify nitrification by crenarchaeal relatives of *N. maritimus* as a dominant energy source in the upper OMZ (in late autumn 2008), suggesting this group as a candidate for more intensive taxon-specific genomic analyses over temporal gradients. Additionally, together with other recent analyses (Lavik *et al.*, 2009; Walsh *et al.*, 2009; Canfield *et al.*, 2010), our results indicate the presence of an active sulfur-oxidizing community in the Chilean OMZ, showing the expression of a diverse set of dissimilatory sulfur oxidation genes and identifying a South Pacific relative of the SUP05 lineage as a dominant and active component of the OMZ community with potential direct ties to the denitrification pathway. However, dominant trends were highlighted here at the expense of more cryptic, but potentially equally important, patterns that could not be adequately addressed in a single study (e.g. carbon-fixation pathways). These datasets therefore provide a reference point for more targeted follow-up studies of specific pathways, ideally involving hypotheses that can be tested through direct experimentation or corroborated by metabolic rate measurements. As more metatranscriptome datasets become available, the integration of these and other data will facilitate comparative studies exploring fundamental features of microbial gene expression that occur across dynamic redox gradients.

Experimental procedures

Sample collection

Microbial community DNA and RNA samples were collected from the ETSP OMZ as part of the Microbial Oceanography of Oxygen Minimum Zones (MOOMZ-1) cruise aboard the *R/V Vidal Gormaz* (June 12–23, 2008). Seawater was sampled from four depths (50, 85, 110, 200 m) at Station #3 (20°07'S, 70°23'W; ~1050 m water depth; Fig. S1A) off the coast of Iquique, Chile on June 16–17 using 10 l Niskin bottles deployed on a rosette system containing a conductivity-temperature-depth profiler (Seabird 25; Seabird Electronics) equipped with an Optode dissolved oxygen sensor. Replicate seawater samples for RNA extraction ($n=4$ replicates; 1.5–3.0 l seawater per replicate) were pre-filtered through 1.6 µm GF/A filters (47 mm dia., Whatman) and collected onto 0.22 µm Durapore filters (25 mm dia., Millipore) using a peristaltic pump (1.5–3.0 l seawater per filter). Filters were immediately transferred to microcentrifuge tubes containing 300 µl RNeasy Lysis Buffer (Qiagen) and frozen at –80°C, with less than 15 min elapsing between sample collection (arrival on deck) and fixation in RNeasy Lysis Buffer. Samples for DNA extraction were collected from the same water sample used for RNA collection, as in Frias-Lopez and colleagues (2008). For each sample, seawater (15–30 l) was filtered through a 1.6 µm GF/A prefilter (125 mm dia., Whatman) and then collected on a 0.22 µm Steripak-GP20 filter (Millipore). The filter units were filled with lysis buffer (50 mM Tris-HCl, 40 mM EDTA, and 0.75 M sucrose), capped and frozen at –80°C until extraction.

RNA and DNA isolation

Total RNA was extracted from filters using a modification of the *mirVana* miRNA Isolation kit (Ambion) as described previously (Shi *et al.*, 2009; Stewart *et al.*, 2010). Briefly, samples were thawed on ice, and the RNeasy Lysis Buffer surrounding each filter was removed and discarded. Filters were immersed in Lysis/Binding buffer (Ambion) and vortexed to lyse attached cells. Total RNA was then extracted from the lysate according to the manufacturer's protocol, incubated (37°C for 30 min) with TURBO DNA-free to remove genomic DNA, and purified and concentrated using the RNeasy MinElute Cleanup kit (Qiagen). Genomic DNA was extracted from Steripak filters as described previously (Frias-Lopez *et al.*, 2008).

rRNA subtraction, RNA amplification and cDNA synthesis

The proportion of bacterial ribosomal RNA transcripts (16S and 23S molecules) in total RNA extracts was reduced via a subtractive hybridization protocol using sample-specific rRNA probes, as described in Stewart and colleagues (2010). rRNA-depleted total RNA (~35–100 ng) was then amplified using the MessageAmp II-Bacteria kit (Ambion) as described previously (Frias-Lopez *et al.*, 2008; Shi *et al.*, 2009). Briefly, total RNA was polyadenylated using *Escherichia coli* poly(A) polymerase. Polyadenylated RNA was converted to double-

stranded cDNA via reverse transcription primed with an oligo(dT) primer containing a promoter sequence for T7 RNA polymerase and a recognition site for the restriction enzyme BpmI (T7-BpmI-(dT)₁₆VN). cDNA was then transcribed *in vitro* at 37°C (12–14 h), yielding large quantities (20–110 µg) of single-stranded antisense RNA. Amplified RNA (~5–10 µg aliquot) was then converted to double-stranded cDNA using the SuperScript® III First-Strand Synthesis System (Invitrogen) with priming via random hexamers for first-stranded synthesis, and the SuperScript Double-Stranded cDNA synthesis kit (Invitrogen) for second-stranded synthesis. cDNA was then purified with the QIAquick PCR purification kit (Qiagen), digested with BpmI for 2–3 h at 37°C to remove poly(A) tails, and used directly for pyrosequencing.

Pyrosequencing

Poly(A)-removed cDNA was purified for sequencing via the AMPure® kit (Agencourt®) and used for the generation of single-stranded DNA libraries and emulsion PCR according to established protocols (454 Life Sciences, Roche). Clonally amplified library fragments were sequenced with full plate runs on a Roche Genome Sequencer FLX instrument (excluding the 85 m cDNA sample, which was sequenced on a half plate).

Data analysis

Sequences sharing 100% nucleotide similarity and length (replicates) may represent artefacts generated by preparing samples for pyrosequencing (Gomez-Alvarez *et al.*, 2009; Stewart *et al.*, 2010). Replicates were identified among non-rRNA sequences using the open-source programme CD-HIT (Li and Godzik, 2006) and removed from each dataset. Non-replicate reads matching ribosomal RNA genes were identified in cDNA and DNA datasets by BLASTN comparisons with a database containing prokaryotic and eukaryotic small and large subunit rRNA nucleotide sequences (5S, 16S, 18S, 23S and 28S rRNA) compiled from microbial genomes and sequences in the ARB SILVA LSU and SSU databases (<http://www.arb-silva.de>). Reads aligning with bit scores > 50 were identified as rRNA sequences and removed. Small subunit ribosomal RNA reads (16S) from the DNA-based datasets were characterized according to the NCBI taxonomy based on alignments obtained through the greengenes workbench (<http://greengenes.lbl.gov>: Fig. S5).

Non-replicate, non-rRNA sequences were characterized by homology searches (BLASTX) against the National Center for Biotechnology Information non-redundant protein database (NCBI-nr, as of November 26, 2009) and the Kyoto Encyclopedia of Genes and Genomes (KEGG, as of February 2009). The top reference gene(s) matching each read (bit score cut-off = 50) was used for NCBI-nr and KEGG annotations. For reads matching multiple reference genes with equal bit score, each matching reference gene was retained as a top hit, with its representation scaled proportionately to the number of genes sharing an equal bit score. The relative transcriptional activity for a given gene was normalized to account for variations in gene abundance in the DNA pool and is presented as an expression ratio for each dataset:

(RNA reads per gene/total RNA reads matching genes)/
(DNA reads per gene/total DNA reads matching genes).

Read counts across KEGG categories were used to cluster datasets based on shared gene content. For each sample, hit counts per KEGG category were normalized to the percentage of total reads matching the KEGG database. Pearson correlation coefficients were calculated for each pair of normalized datasets and used as similarity indices for hierarchical clustering based on the complete linkage method, as implemented in Cluster 3.0. The same analysis was repeated using read counts per unique nr taxonomic identifier as relatedness criteria, with the number of unique taxonomic identifiers per dataset standardized across datasets (mean = 1885 taxa; stdev = 0.3%).

Nucleotide sequence data generated in this study are available in the NCBI Sequence Read Archive under accession number SRA023632.1.

Acknowledgements

This work was supported by a grant from the Agouron Institute. We thank Sara Lincoln, J. Francisco Santibáñez, Gadiel Alarcón, and the captain and crew of the *Vidal Gormaz* for their help in collecting samples for this study, Jay McCarren for help with sample collection, DNA extractions and metagenomic analysis, and Rachel Barry for her tireless work in preparing samples for pyrosequencing. Finally, we thank three anonymous reviewers for their thoughtful and constructive comments on this work. Additional support for this study came from the Gordon and Betty Moore Foundation (EFD), the Office of Science (BER) US Department of Energy, and the Chilean Fondap Program (OU). This work is a contribution of the Center for Microbial Oceanography: Research and Education (C-MORE).

References

- Andrade, S.L.A., and Einsle, O. (2007) The Amt/Mep/Rh family of ammonium transport proteins. *Mol Membr Biol* **24**: 357–365.
- Canfield, D.E., Stewart, F.J., Thamdrup, B., De Brabandere, L., Dalsgaard, T., DeLong, E.F., *et al.* (2010) A cryptic sulfur cycle in oxygen-minimum-zone waters off the Chilean coast. *Science* **330**: 1375–1378.
- Carlson, C.A., Morris, R., Parsons, R., Treusch, A.H., Giovannoni, S.J., and Vergin, K. (2009) Seasonal dynamics of SAR11 populations in the euphotic and mesopelagic zones of the northwestern Sargasso Sea. *ISME J* **3**: 283–295.
- Castro-González, M., Braker, G., Farias, L., and Ulloa, O. (2005) Communities of nirS-type denitrifiers in the water column of the oxygen minimum zone in the eastern South Pacific. *Environ Microbiol* **7**: 1298–1306.
- Church, M.J., Wai, B., Karl, D.M., and DeLong, E.F. (2010) Abundances of crenarchaeal amoA genes and transcripts in the Pacific Ocean. *Environ Microbiol* **12**: 679–688.
- Codispoti, L.A., Brandes, J.A., Christensen, J.P., Devol, A.H., Naqvi, S.W.A., Paerl, H.W., and Yoshinari, T. (2001) The oceanic fixed nitrogen and nitrous oxide budgets: moving targets as we enter the anthropocene? *Sci Mar* **65**: 85–105.

- Daneri, G., Dellarossa, V., Quiñones, R., Jacob, B., Montero, P., and Ulloa, O. (2000) Primary production and community respiration in the Humboldt Current System off Chile and associated oceanic areas. *Mar Ecol Prog Ser* **197**: 41–49.
- DeLong, E.F., Preston, C.M., Mincer, T., Rich, V., Hallam, S.J., Frigaard, N.U., *et al.* (2006) Community genomics among stratified microbial assemblages in the ocean's interior. *Science* **311**: 496–503.
- Dhillon, A., Goswami, S., Riley, M., Teske, A., and Sogin, M. (2005) Domain evolution and functional diversification of sulfite reductases. *Astrobiology* **5**: 18–29.
- Diaz, R.J., and Rosenberg, R. (2008) Spreading dead zones and consequences for marine ecosystems. *Science* **321**: 926–929.
- Erguder, T.H., Boon, N., Wittebolle, L., Marzorati, M., and Verstraete, W. (2009) Environmental factors shaping the ecological niches of ammonia-oxidizing archaea. *FEMS Microbiol Rev* **33**: 855–869.
- Fariás, L., Paulmier, A., and Gallegos, M. (2007) Nitrous oxide and N-nutrient cycling in the oxygen minimum zone off northern Chile. *Deep Sea Res Part I Oceanogr Res Pap* **54**: 164–180.
- Fariás, L., Castro-González, M., Cornejo, M., Charpentier, J., Faúndez, J., Boontanon, N., and Yoshida, N. (2009) Denitrification and nitrous oxide cycling within the upper oxycline of the eastern tropical South Pacific oxygen minimum zone. *Limnol Oceanogr* **54**: 132–144.
- Frias-Lopez, J., Shi, Y., Tyson, G.W., Coleman, M.L., Schuster, S.C., Chisholm, S.W., and DeLong, E.F. (2008) Microbial community gene expression in ocean surface waters. *Proc Natl Acad Sci USA* **105**: 3805–3810.
- Fuchs, B.M., Woebken, D., Zubkov, M.V., Burkill, P., and Amann, R. (2005) Molecular identification of picoplankton populations in contrasting waters of the Arabian Sea. *Aquat Microb Ecol* **39**: 145–157.
- Galán, A., Molina, V., Thamdrup, B., Woebken, D., Lavik, G., Kuypers, M.M.M., and Ulloa, O. (2009) Anammox bacteria and the anaerobic oxidation of ammonium in the oxygen minimum zone off northern Chile. *Deep Sea Res Part II Top Stud Oceanogr* **56**: 1021–1031.
- Gomez-Alvarez, V., Teal, T.K., and Schmidt, T.M. (2009) Systematic artifacts in metagenomes from complex microbial communities. *ISME J* **3**: 1314–1317.
- Hallam, S.J., Konstantinidis, K.T., Putnam, N., Schleper, C., Watanabe, Y., Sugahara, J., *et al.* (2006a) Genomic analysis of the uncultivated marine crenarchaeote *Cenarchaeum symbiosum*. *Proc Natl Acad Sci USA* **103**: 18296–18301.
- Hallam, S.J., Mincer, T.J., Schleper, C., Preston, C.M., Roberts, K., Richardson, P.M., and DeLong, E.F. (2006b) Pathways of carbon assimilation and ammonia oxidation suggested by environmental genomic analyses of marine *Crenarchaeota*. *PLoS Biol* **4**: 520–536.
- Hamersley, M.R., Lavik, G., Woebken, D., Rattray, J.E., Lam, P., Hopmans, E.C., *et al.* (2007) Anaerobic ammonium oxidation in the Peruvian oxygen minimum zone. *Limnol Oceanogr* **52**: 923–933.
- Hewson, I., Poretsky, R.S., Beinart, R.A., White, A.E., Shi, T., Bench, S.R., *et al.* (2009) *In situ* transcriptomic analysis of the globally important keystone N₂-fixing taxon *Crocospaera watsonii*. *ISME J* **3**: 618–631.
- Hewson, I., Poretsky, R.S., Tripp, H.J., Montoya, J.P., and Zehr, J.P. (2010) Spatial patterns and light-driven variation of microbial population gene expression in surface waters of the oligotrophic open ocean. *Environ Microbiol* **12**: 1940–1956.
- Jayakumar, A., O'Mullan, G.D., Naqvi, S.W.A., and Ward, B.B. (2009) Denitrifying bacterial community composition changes associated with stages of denitrification in oxygen minimum zones. *Microb Ecol* **58**: 350–362.
- Jensen, M.M., Petersen, J., Dalsgaard, T., and Thamdrup, B. (2009) Pathways, rates, and regulation of N₂ production in the chemocline on an anoxic basin, Mariager Fjord, Denmark. *Mar Chem* **113**: 102–113.
- Jetten, M.S.M., van Niftrik, L., Strous, M., Kartal, B., Keltjens, J.T., and Op den Camp, H.J.M. (2009) Biochemistry and molecular biology of anammox bacteria. *Crit Rev Biochem Mol Biol* **44**: 65–84.
- Kartal, B., Kuypers, M.M.M., Lavik, G., Schalk, J., den Camp, H.J.M.O., Jetten, M.S.M., and Strous, M. (2007a) Anammox bacteria disguised as denitrifiers: nitrate reduction to dinitrogen gas via nitrite and ammonium. *Environ Microbiol* **9**: 635–642.
- Kartal, B., Rattray, J., van Niftrik, L.A., van de Vossenberg, J., Schmid, M.C., Webb, R.I., *et al.* (2007b) Candidatus '*Anammoxoglobus propionicus*' a new propionate oxidizing species of anaerobic ammonium oxidizing bacteria. *Syst Appl Microbiol* **30**: 39–49.
- Kartal, B., van Niftrik, L., Rattray, J., de Vossenberg, J.L.C.M.V., Schmid, M.C., Damste, J.S.S., *et al.* (2008) Candidatus '*Brocadia fulgida*': an autofluorescent anaerobic ammonium oxidizing bacterium. *FEMS Microbiol Ecol* **63**: 46–55.
- Konneke, M., Bernhard, A.E., de la Torre, J.R., Walker, C.B., Waterbury, J.B., and Stahl, D.A. (2005) Isolation of an autotrophic ammonia-oxidizing marine archaeon. *Nature* **437**: 543–546.
- Konstantinidis, K.T., Braff, J., Karl, D.M., and DeLong, E.F. (2009) Comparative Metagenomic Analysis of a Microbial Community Residing at a Depth of 4,000 Meters at Station ALOHA in the North Pacific Subtropical Gyre. *Appl Environ Microbiol* **75**: 5345–5355.
- Kuenen, J.G. (2008) Anammox bacteria: from discovery to application. *Nat Rev Microbiol* **6**: 320–326.
- Kuwahara, H., Yoshida, T., Takaki, Y., Shimamura, S., Nishi, S., Harada, M., *et al.* (2007) Reduced genome of the thioautotrophic intracellular symbiont in a deep-sea clam, *Calyptogena okutanii*. *Curr Biol* **17**: 881–886.
- Kuypers, M.M.M., Sliekers, A.O., Lavik, G., Schmid, M., Jorgensen, B.B., Kuenen, J.G., *et al.* (2003) Anaerobic ammonium oxidation by anammox bacteria in the Black Sea. *Nature* **422**: 608–611.
- Kuypers, M.M.M., Lavik, G., Woebken, D., Schmid, M., Fuchs, B.M., Amann, R., *et al.* (2005) Massive nitrogen loss from the Benguela upwelling system through anaerobic ammonium oxidation. *Proc Natl Acad Sci USA* **102**: 6478–6483.
- Labrenz, M., Sintes, E., Toetzke, F., Zumsteg, A., Herndl, G.J., Seidler, M., and Jürgens, K. (2010) Relevance of a crenarchaeotal subcluster related to Candidatus *Nitrosopumilus maritimus* to ammonia oxidation in the suboxic zone of the central Baltic Sea. *ISME J* **4**: 1496–1508.

- Lam, P., Jensen, M.M., Lavik, G., McGinnis, D.F., Muller, B., Schubert, C.J., *et al.* (2007) Linking crenarchaeal and bacterial nitrification to anammox in the Black Sea. *Proc Natl Acad Sci USA* **104**: 7104–7109.
- Lam, P., Lavik, G., Jensen, M.M., van de Vossenberg, J., Schmid, M., Woebken, D., *et al.* (2009) Revising the nitrogen cycle in the Peruvian oxygen minimum zone. *Proc Natl Acad Sci USA* **106**: 4752–4757.
- Lavik, G., Stuhmann, T., Bruchert, V., Van der Plas, A., Mohrholz, V., Lam, P., *et al.* (2009) Detoxification of sulphidic African shelf waters by blooming chemolithotrophs. *Nature* **457**: 581–584.
- Leigh, J.A., and Dodsworth, J.A. (2007) Nitrogen regulation in bacteria and archaea. *Annu Rev Microbiol* **61**: 349–377.
- Li, W.Z., and Godzik, A. (2006) Cd-hit: a fast program for clustering and comparing large sets of protein or nucleotide sequences. *Bioinformatics* **22**: 1658–1659.
- McCarren, J., Becker, J.W., Repeta, D.J., Shi, Y.M., Young, C.R., Malmstrom, R.R., *et al.* (2010) Microbial community transcriptomes reveal microbes and metabolic pathways associated with dissolved organic matter turnover in the sea. *Proc Natl Acad Sci USA* **107**: 16420–16427.
- Martens-Habbena, W., Berube, P.M., Urakawa, H., de la Torre, J.R., and Stahl, D.A. (2009) Ammonia oxidation kinetics determine niche separation of nitrifying Archaea and Bacteria. *Nature* **461**: 976–U234.
- Meyer, B., and Kuever, J. (2007a) Molecular analysis of the diversity of sulfate-reducing and sulfur-oxidizing prokaryotes in the environment, using *aprA* as functional marker gene. *Appl Environ Microbiol* **73**: 7664–7679.
- Meyer, B., and Kuever, J. (2007b) Phylogeny of the alpha and beta subunits of the dissimilatory adenosine-5'-phosphosulfate (APS) reductase from sulfate-reducing prokaryotes – origin and evolution of the dissimilatory sulfate-reduction pathway. *Microbiology* **153**: 2026–2044.
- Molina, V., and Farías, L. (2009) Aerobic ammonium oxidation in the oxycline and oxygen minimum zone of the eastern tropical South Pacific off northern Chile (similar to 20 degrees S). *Deep Sea Res Part II Top Stud Oceanogr* **56**: 1032–1041.
- Molina, V., Farías, L., Eissler, Y., Cuevas, L.A., Morales, C.E., and Escribano, R. (2005) Ammonium cycling under a strong oxygen gradient associated with the Oxygen Minimum Zone off northern Chile (similar to 23 degrees S). *Mar Ecol Prog Ser* **288**: 35–43.
- Molina, V., Ulloa, O., Farías, L., Urrutia, H., Ramirez, S., Junier, P., and Witzel, K.P. (2007) Ammonia-oxidizing beta-Proteobacteria from the oxygen minimum zone off northern Chile. *Appl Environ Microbiol* **73**: 3547–3555.
- Molina, V., Belmar, L., and Ulloa, O. (2010) High diversity of ammonia-oxidizing archaea in permanent and seasonal oxygen-deficient waters of the eastern South Pacific. *Environ Microbiol* **12**: 2450–2465.
- Newton, I.L.G., Woyke, T., Auchtung, T.A., Dilly, G.F., Dutton, R.J., Fisher, M.C., *et al.* (2007) The *Calyptogenia magnifica* chemoautotrophic symbiont genome. *Science* **315**: 998–1000.
- Poretsky, R.S., Hewson, I., Sun, S.L., Allen, A.E., Zehr, J.P., and Moran, M.A. (2009) Comparative day/night metatranscriptomic analysis of microbial communities in the North Pacific subtropical gyre. *Environ Microbiol* **11**: 1358–1375.
- Poretsky, R.S., Sun, S.L., Mou, X.Z., and Moran, M.A. (2010) Transporter genes expressed by coastal bacterioplankton in response to dissolved organic carbon. *Environ Microbiol* **12**: 616–627.
- Preston, C.M., Wu, K.Y., Molinski, T.F., and DeLong, E.F. (1996) A psychrophilic crenarchaeon inhabits a marine sponge: *Cenarchaeum symbiosum* gen nov, sp, nov. *Proc Natl Acad Sci USA* **93**: 6241–6246.
- Prosser, J.I., and Nicol, G.W. (2008) Relative contributions of archaea and bacteria to aerobic ammonia oxidation in the environment. *Environ Microbiol* **10**: 2931–2941.
- Revsbech, N.P., Larsen, L.H., Gundersen, J., Dalsgaard, T., Ulloa, O., and Thamdrup, B. (2009) Determination of ultra-low oxygen concentrations in oxygen minimum zones by the STOX sensor. *Limnol Oceanogr Methods* **7**: 371–381.
- Schleper, C., Jurgens, G., and Jonuscheit, M. (2005) Genomic studies of uncultivated archaea. *Nat Rev Microbiol* **3**: 479–488.
- Schmidt, I., Look, C., Bock, E., and Jetten, M.S.M. (2004) Ammonium and hydroxylamine uptake and accumulation in Nitrosomonas. *Microbiology* **150**: 1405–1412.
- Shi, Y.M., Tyson, G.W., and DeLong, E.F. (2009) Metatranscriptomics reveals unique microbial small RNAs in the ocean's water column. *Nature* **459**: 266–269.
- Snel, B., Bork, P., and Huynen, M.A. (1999) Genome phylogeny based on gene content. *Nat Genet* **21**: 108–110.
- Sowell, S.M., Wilhelm, L.J., Norbeck, A.D., Lipton, M.S., Nicora, C.D., Barofsky, D.F., *et al.* (2009) Transport functions dominate the SAR11 metaproteome at low-nutrient extremes in the Sargasso Sea. *ISME J* **3**: 93–105.
- Stevens, H., and Ulloa, O. (2008) Bacterial diversity in the oxygen minimum zone of the eastern tropical South Pacific. *Environ Microbiol* **10**: 1244–1259.
- Stewart, F.J., Ottesen, E.A., and DeLong, E.F. (2010) Development and quantitative analyses of a universal rRNA-subtraction protocol for microbial metatranscriptomics. *ISME J* **4**: 896–907.
- Stramma, L., Johnson, G.C., Sprintall, J., and Mohrholz, V. (2006) Expanding oxygen-minimum zones in the tropical oceans. *Science* **320**: 655–658.
- Strous, M., Pelletier, E., Mangenot, S., Rattai, T., Lehner, A., Taylor, M.W., *et al.* (2006) Deciphering the evolution and metabolism of an anammox bacterium from a community genome. *Nature* **440**: 790–794.
- Taniguchi, Y., Choi, P.J., Li, G.W., Chen, H.Y., Babu, M., Hearn, J., *et al.* (2010) Quantifying e-coli proteome and transcriptome with single-molecule sensitivity in single cells. *Science* **329**: 533–538.
- Thamdrup, B., Dalsgaard, T., Jensen, M.M., Ulloa, O., Farías, L., and Escribano, R. (2006) Anaerobic ammonium oxidation in the oxygen-deficient waters off northern Chile. *Limnol Oceanogr* **51**: 2145–2156.
- Ulloa, O., and Pantoja, S. (2009) The oxygen minimum zone of the eastern South Pacific. *Deep Sea Res Part II Top Stud Oceanogr* **56**: 987–991.
- Urich, T., Lanzen, A., Qi, J., Huson, D.H., Schleper, C., and Schuster, S.C. (2008) Simultaneous assessment of soil microbial community structure and function through analysis of the meta-transcriptome. *PLoS ONE* **3**: e2527.
- Walker, C.B., de la Torre, J.R., Klotz, M.G., Urakawa, H., Pinel, N., Arp, D.J., *et al.* (2010) *Nitrosopumilus maritimus*

- genome reveals unique mechanisms for nitrification and autotrophy in globally distributed marine crenarchaea. *Proc Natl Acad Sci USA* **107**: 8818–8823.
- Walsh, D.A., Zaikova, E., Howes, C.G., Song, Y.C., Wright, J.J., Tringe, S.G., *et al.* (2009) Metagenome of a versatile chemolithoautotroph from expanding oceanic dead zones. *Science* **326**: 578–582.
- Ward, B.B., Devol, A.H., Rich, J.J., Chang, B.X., Bulow, S.E., Naik, H., *et al.* (2009) Denitrification as the dominant nitrogen loss process in the Arabian Sea. *Nature* **461**: 78–81.
- Weidinger, K., Neuhauser, B., Gilch, S., Ludewig, U., Meyer, O., and Schmidt, I. (2007) Functional and physiological evidence for a Rhesus-type ammonia transporter in *Nitrosomonas europaea*. *FEMS Microbiol Lett* **273**: 260–267.
- Woebken, D., Lam, P., Kuypers, M.M.M., Naqvi, S.W.A., Kartal, B., Strous, M., *et al.* (2008) A microdiversity study of anammox bacteria reveals a novel Candidatus Scalindua phylotype in marine oxygen minimum zones. *Environ Microbiol* **10**: 3106–3119.
- Wuchter, C., Abbas, B., Coolen, M.J.L., Herfort, L., van Bleijswijk, J., Timmers, P., *et al.* (2006) Archaeal nitrification in the ocean. *Proc Natl Acad Sci USA* **103**: 12317–12322.
- Zaikova, E., Walsh, D.A., Stilwell, C.P., Mohn, W.W., Tortell, P.D., and Hallam, S.J. (2010) Microbial community dynamics in a seasonally anoxic fjord: Saanich Inlet, British Columbia. *Environ Microbiol* **12**: 172–191.

Supporting information

Additional Supporting Information may be found in the online version of this article:

Fig. S1. A. Location of the study site off Iquique, Chile (Station #3, boxed; 20°07'S, 70°23'W).

B. Vertical distributions of physical and chemical water properties at Station #3 in June 2008. Oxygen (O₂), photosynthetically active radiation (PAR; time of day: 1215), and temperature (left panel) were sampled via conductivity-temperature-depth (equipped with a dissolved oxygen sensor) on June 16, at the start of the DNA/RNA sample collection (June 16–17). Water for nitrate (NO₃⁻), nitrite (NO₂⁻) and ammonium (NH₄⁺) analyses (right panel) was collected via rosette during a surveying transect on June 14. DNA/RNA sampling depths are marked with dashed lines.

Fig. S2. Representative frequency distribution of 454 read density per gene (unique NCBI-nr reference sequence) in the 50 m DNA and RNA datasets. The vast majority of genes are represented by one or fewer reads in both datasets.

Fig. S3. Frequency distribution of reads matching the 100 most abundant protein-coding reference sequences recovered in BLASTX searches against the NCBI-nr database. Frequency (*y*-axis) is shown as a percentage of the total number of reads with matches in NCBI-nr. Values in the legend are the total percentages represented by the 100 most abundant genes. The total numbers of unique reference sequences per dataset are shown in Table 1 (main text).

Fig. S4. Discrepancies between abundance and expression for two prominent OMZ genera. Dashed lines indicate the relative abundance of DNA reads matching *Nitrosopumilus*

(maritimus) and *Pelagibacter* protein-coding genes (as top hits). Solid lines indicate the expression ratio (RNA/DNA, see main text) averaged across all genes per genus. *Pelagibacter* dominates in DNA abundance, but has significantly lower per gene expression. Error bars are 95% confidence intervals.

Fig. S5. Taxonomic distribution of 16S ribosomal RNA gene fragments in metagenome (DNA) samples at station #3. Putative rRNA-encoding reads were identified via BLASTN searches against a rRNA database composed of both prokaryotic and eukaryotic small and large subunit rRNA nucleotide sequences (5S, 16S, 18S, 23S and 28S rRNA) from available microbial genomes and sequences in the ARB SILVA LSU and SSU databases (<http://www.arb-silva.de>). Reads greater than 100 nt in length that aligned with bit scores greater than 50 were designated as rRNA sequences and identified taxonomically using the program greengenes (<http://greengenes.lbl.gov>) and the NCBI taxonomy hierarchy. Numbers of 16S gene sequences are listed for each sample. DNA data from 15, 65, 500 and 800 m do not have corresponding RNA data and are therefore not the focus of the main text, but are provided here to help contextualize our primary results.

Fig. S6. Abundances of top hits (bit score > 50) within KEGG reference pathways (KEGG 2 hierarchy level) represented in RNA datasets from four depths in the OMZ. Abundance is shown as a percentage of total hits mapping across all KEGG 2 pathways. Orthologues are ordered by rank abundance in the 200 m sample (light blue bars).

Fig. S7. Abundances of top hits (bit score > 50) within KEGG reference pathways (KEGG 3 hierarchy level) represented in RNA datasets from four depths in the OMZ. Abundance is shown as a percentage of total hits mapping across all KEGG 3 pathways. Orthologues are ordered by rank abundance in the 200 m sample (light blue bars).

Fig. S8. Abundances of top hits to KEGG orthologues (bit score > 50) in RNA datasets from four depths in the OMZ, as a percentage of total hits mapping to the KEGG ko hierarchy. The figure shows only orthologues for which the percentage of total hits exceeds 0.25% in at least one of the four datasets. Orthologues are ordered by rank abundance in the 200 m sample (light blue bars). Gray shading marks proteins with putative transport functions. Red marks proteins of nitrogen metabolism or transport. Green marks proteins of photosynthesis and carbon fixation. Note: ammonia monooxygenase subunit genes (*amoABC*) predominantly matched the archaeal genes of *Nitrosopumilus maritimus* [Nmar_1500 (*amoA*), Nmar_1502 (*amoC*), Nmar_1503 (*amoB*)], which did not have an associated ko identifier and did not parse automatically to the ko hierarchy; these reads were manually extracted from the KEGG BLAST results and added to the totals shown here.

Fig. S9. Abundance and taxonomic classification of sequencing reads that match genes encoding Amt-like ammonium transporters and the subunits of ammonia monooxygenase (*amoA*, *B*, *C* combined). Abundance is shown as a percentage of total sequencing reads with matches in NCBI-nr. Pie charts show the proportion of bacterial, archaeal, or unclassified *amt* or *amo* sequences at each depth, based on annotations in NCBI-nr. *Amt* and *amo* are represented by a mixture of bacteria and archaea sequences in the DNA pool, but are dominated by archaea in the expressed gene pool.

Fig. S10. Diversity and abundance of sequencing reads matching *narG*, encoding the alpha subunit of the dissimilatory nitrate reductase. Colours and numbers (lower right for each chart) reflect distinct *narG* reference sequences in the NCBI-nr database, with the colours for the four most abundance reference taxa (legend) consistent across charts. Chart area reflects the relative abundance of reads matching *narG* (as the top hit) as a proportion of the total number of reads (in each dataset) with matches in NCBI-nr, peaking at 1.1% in the 200 m RNA sample from the core of the OMZ.

Fig. S11. Transposase abundance increases with depth. OMZ DNA and RNA reads matching transposase genes in NCBI-nr are shown as a percentage of total reads matching the NCBI-nr database. Transposase content in metagenomes along a 4000 m depth profile in the North Pacific Subtropical Gyre (Station ALOHA, Hawaii Ocean Time-Series, HOTS) is shown for comparison, with transposase abundance as a proportion of total gene content in fosmid libraries (see fig. 3 in Konstantinidis *et al.*, 2009, AEM 75:5345–5355). Note variation in depth scales.

Table S1. Total shared gene content across datasets.

Table S2. Common NCBI-nr content in 454 datasets.

Table S3. Top 10 most abundant genes (protein-coding RNA) from four prominent OMZ taxa (Fig. 5, main text).

Table S4. Top 10 most highly expressed genes from four prominent OMZ taxa (Fig. 5, main text).

Table S5. Top genes identified via BLASTX comparisons with KEGG orthologue and NCBI-nr databases, ranked by expression ratio (exp) and transcript abundance (abun).

Table S6. Proportional abundance and expression of select nitrogen and sulfur metabolism genes.

Table S7. Taxonomic representation and abundance of dissimilatory APS reductase subunit A (*aprA*) genes.

Table S8. Taxonomic distribution and abundance of dissimilatory sulfite reductase (*dsr*) genes.

Please note: Wiley-Blackwell are not responsible for the content or functionality of any supporting materials supplied by the authors. Any queries (other than missing material) should be directed to the corresponding author for the article.